The Plant Cell, Vol. 26: 4214–4229, October 2014, www.plantcell.org

Critical Function of a *Chlamydomonas reinhardtii* Putative Polyphosphate Polymerase Subunit during Nutrient Deprivation[C][W]

Munevver Aksoy,[a,1] Wirulda Pootakham,[a,b] and Arthur R. Grossman[a]

[a] The Carnegie Institution for Science, Department of Plant Biology, Stanford, California 94305
[b] National Center for Genetic Engineering and Biotechnology, Pathum Thani 12120, Thailand

Forward genetics was used to isolate *Chlamydomonas reinhardtii* mutants with altered abilities to acclimate to sulfur (S) deficiency. The *ars76* mutant has a deletion that eliminates several genes, including *VACUOLAR TRANSPORTER CHAPERONE1* (*VTC1*), which encodes a component of a polyphosphate polymerase complex. The *ars76* mutant cannot accumulate arylsulfatase protein or mRNA and shows marked alterations in levels of many transcripts encoded by genes induced during S deprivation. The mutant also shows little acidocalcisome formation compared with wild-type, S-deprived cells and dies more rapidly than wild-type cells following exposure to S-, phosphorus-, or nitrogen (N)-deficient conditions. Furthermore, the mutant does not accumulate periplasmic L-amino acid oxidase during N deprivation. Introduction of the *VTC1* gene specifically complements the *ars76* phenotypes, suggesting that normal acidocalcisome formation in cells deprived of S requires VTC1. Our data also indicate that a deficiency in acidocalcisome function impacts trafficking of periplasmic proteins, which can then feed back on the transcription of the genes encoding these proteins. These results and the reported function of vacuoles in degradation processes suggest a major role of the acidocalcisome in reshaping the cell during acclimation to changing environmental conditions.

INTRODUCTION

The sulfate anion (SO_4^{2-}) is usually the dominant form of sulfur (S) in the environment and is also the most oxidized S species. Animals do not have the enzymatic machinery needed for reducing SO_4^{2-} to sulfide (S^{2-}), which is required to synthesize most S-containing compounds. Plants and microbes have specific transporters that efficiently import SO_4^{2-} into cells, where it is activated, reduced, and then incorporated into S-containing amino acids and other key molecules, including *S*-adenosylmethionine (SAM), GSH, FeS clusters, thionucleosides, sulfolipids, vitamins, and different enzyme cofactors like CoA, molybdoprotein, thiamine, or biotin. However, most organisms have a low capacity to store S, although they have generally developed diverse acclimation strategies that optimize S utilization and balance the rate of S metabolism with S availability; these processes allow organisms to maintain viability even when S is severely limiting to growth.

The unicellular green alga *Chlamydomonas reinhardtii* (*Chlamydomonas* throughout) has been a powerful model organism for dissecting responses of photosynthetic eukaryotes to nutrient deprivation, including deprivation for iron (Blaby-Haas and Merchant, 2012; Page et al., 2012; Urzica et al., 2012, 2013; Hsieh et al., 2013), nitrogen (N) (Miller et al., 2010; Boyle et al., 2012; Blaby et al., 2013), and phosphorus (P) (Moseley et al., 2006, 2009; Yehudai-Resheff et al., 2007; Moseley and Grossman, 2009), and S (Moseley et al., 2009; González-Ballester et al., 2010; Cakmak et al., 2012a, 2012b; Aksoy et al., 2013; Schmollinger et al., 2014). Processes induced by S deprivation in this alga include rapid changes in cell size (Zhang et al., 2002), elevated production of hydrolytic extracellular enzymes (de Hostos et al., 1988; Takahashi et al., 2001), alterations in cell wall structure (Takahashi et al., 2001), changes in the activities and composition of the photosynthetic apparatus (Collier and Grossman, 1992; Wykoff et al., 1998; Zhang et al., 2004; Moseley et al., 2009; González-Ballester et al., 2010; Cakmak et al., 2012a, 2012b; Aksoy et al., 2013), scavenging of S from intracellular structures/molecules, elevated SO_4^{2-} transport activity (Yildiz et al., 1994; Pootakham et al., 2010), and the synthesis of enzymes required for efficient S assimilation (Ravina et al., 1999, 2002; González-Ballester et al., 2010). Moreover, S-depleted *Chlamydomonas* cells have been used for microarray- and RNA-seq-based transcript abundance studies (Zhang et al., 2004; Nguyen et al., 2008; González-Ballester et al., 2010), determination of metabolite profiles (Bölling and Fiehn, 2005), and the production of H_2 (Ghirardi et al., 2007). Numerous studies of S-deprived plants have also been performed (Lewandowska and Sirko, 2008; Kopriva et al., 2009; Lee et al., 2012; Ciaffi et al., 2013), with some of these that include determinations of transcript levels and metabolite profiles (Hirai et al., 2003; Maruyama Nakashita et al., 2003; Nikiforova et al., 2005a, 2005b; Lunde et al., 2008; Kopriva et al., 2012).

Over the last decade a number of regulatory elements controlling S deprivation responses in *Chlamydomonas* have been

[1] Address correspondence to maksoy1@stanford.edu.
The author responsible for distribution of materials integral to the findings presented in this article in accordance with the policy described in the Instructions for Authors (www.plantcell.org) is: Munevver Aksoy (maksoy1@stanford.edu).
[C] Some figures in this article are displayed in color online but in black and white in the print edition.
[W] Online version contains Web-only data.
www.plantcell.org/cgi/doi/10.1105/tpc.114.129270

identified. The *SULFUR ACCLIMATION1* (*SAC1*) gene encodes a polypeptide with homology to Na^+/SO_4^{2-} transporters (SLC13 family), but it appears to function as a sensor that responds to extracellular SO_4^{2-} levels (Davies et al., 1996; Moseley et al., 2009). The *sac1* mutant exhibits a marked reduction in accumulation of many transcripts encoding proteins associated with S deprivation responses (Takahashi et al., 2001; Ravina et al., 2002; Zhang et al., 2004) and rapidly loses viability when it is exposed to medium devoid of S. This loss of viability may be the consequence of the inability of the cells to decrease photosynthetic electron transport activity following depletion of S from the medium (Wykoff et al., 1998). However, transcription from some S-responsive genes does not show an absolute dependence on SAC1. For example, the *sac1* mutant still develops a significant level of high affinity SO_4^{2-} transport activity (Davies et al., 1996) and accumulates transcripts encoding SO_4^{2-} transporters in response to S deprivation (Gonzalez-Ballester et al., 2008). Recently, it was suggested that SAC1 acts as a negative modulator of the activity of the regulatory kinase SNRK2.2 (see below) during S deprivation (Moseley et al., 2009).

Two genes that encode regulatory proteins associated with S deprivation responses and that have been extensively characterized are the plant-specific type 2 SNF1-related serine-threonine kinases *SNRK2.1* and *SNRK2.2* (the latter is also known as *SAC3*) (Davies et al., 1999; González-Ballester et al., 2008, 2010). SNRK2.2 is responsible for repression of S-inducible genes when cells are replete for S (Davies et al., 1999; Ravina et al., 2002; Gonzalez-Ballester et al., 2008) and may also be involved in repression of chloroplast transcription during S deprivation (Irihimovitch and Stern, 2006). The SNRK2.1 kinase is required for most S-responsive gene expression and for maintaining cell viability during S deprivation. S-responsive gene expression and cell viability are more severely impacted in the *snrk2.1* mutant than in the *sac1* mutant (Pollock et al., 2005; Gonzalez-Ballester et al., 2008). Moreover, while SAC1 and SNRK2.2 do not show a clear epistatic relationship, SNRK2.1 is epistatic to SNRK2.2. Finally, it was demonstrated that there are two levels of control associated with S deprivation responses. The first level does not require protein synthesis, while the second requires protein synthesis as well as the regulatory element ARS73a; this element appears to be specific to a second tier of gene regulation controlled by the S status of the environment (Aksoy et al., 2013).

Recently, RNA-seq was used to evaluate responses of wild-type cells and the *snrk2.1* mutant of *Chlamydomonas* to S deprivation (González-Ballester et al., 2010). This work demonstrated that transcripts for many proteins (and at the protein level for some) associated with the scavenging of SO_4^{2-}, including arylsulfatases (ARSs), specific SO_4^{2-} transporters (SLT1, SLT2, and SULTR2), and potentially transporters of S-containing amino acids (AOT4), accumulate during S deprivation. Moreover, there are transcripts encoding enzymes involved in S assimilation and the synthesis of S metabolites that show either little change in abundance or that decline under S-depleted conditions. For example, transcripts encoding three isoforms of the *O*-acetylserine (thiol)-lyase (OASTL1, OASTL2, and OASTL3), APS kinase, APS reductase, sulfite reductase (SIR3), SAT2, and enzymes required for glutathione synthesis and degradation did not significantly change when the cells were deprived of S. Interestingly, transcripts encoding proteins required for the methionine/SAM cycle and the biosynthesis of the S-containing cofactors thiamine and biotin decreased in abundance under S-depleted conditions, and this decrease is not under SNRK2.1 control. SAM potentially represents a large drain on the methionine pool; 80% of the methionine synthesized in *Lemna paucicostata* cells may be consumed in the SAM pathway, with only ~20% routed to protein synthesis (Giovanelli et al., 1985). Hence, reduced levels of SAM may impact several metabolic pathways including those responsible for the synthesis of thiamine, chlorophyll, polyamines, and lipids. Similarly, the level of an *Arabidopsis thaliana* transcript encoding a protein that likely functions in thiamine biosynthesis was diminished when the organism was deprived of S (Maruyama-Nakashita et al., 2003).

In this study, we characterized a *Chlamydomonas* mutant, designated *ars76*, isolated in a screen for strains unable to properly acclimate to S deprivation (Pollock et al., 2005). This mutant is defective for accumulation of extracellular ARS and bleaches more rapidly than wild-type cells exposed to S deprivation. The mutant is also aberrant for other nutrient deprivation responses including reduced survival of cells during P deprivation and an inability to accumulate L-amino acid oxidase during N deprivation. The insertion associated with the mutant phenotype caused a 33-kb deletion in chromosome 12 that impacted six gene models. Rescue of the mutant phenotype was achieved by reintroducing one of the deleted genes into mutant cells; the gene effective in complementation encodes the putative VTC1 subunit of the polyphosphate polymerase complex, which has also been called the vacuolar transporter chaperone complex (VTC). While the lesion results in an inability of the cells to acclimate normally to S deprivation, it also impacts acclimation of cells to other nutrient-limiting conditions.

RESULTS

Characteristics of the *ars76* Mutant and Impact on ARS Activity

The *ars76* mutant was isolated in a forward genetic screen for *Chlamydomonas* strains devoid of ARS activity. Transformants were screened for ARS activity under both S-replete and S-deficient conditions by spraying the chromogenic substrate 5-bromo-4-chloro-3-indolyl sulfate (X-SO_4^{2-}) onto solid medium (in Petri dishes) on which colonies of transformants were growing (Pollock et al., 2005). The resulting blue color is indicative of ARS activity, which is secreted into the extracellular space (periplasmic space) when wild-type 21 gr *Chlamydomonas* cells are deprived of S (Figure 1A, first and third panels from the left). The original *ars76* mutant, generated in the D66 genetic background, was crossed to wild-type 21 gr to analyze linkage of the paromomycin insertion to the *ars*$^-$ phenotype. In each tetrad, 50% of the progeny were paromomycin resistant (suggesting a single insertion into the genome of *ars76* or closely linked insertions) and the paromomycin resistance and *ars*$^-$ phenotypes cosegregated, indicating that the insertion of the marker gene was linked to the mutant phenotype (Supplemental Figure 1). The mutant was backcrossed three times to wild-type 21 gr and the final progeny assayed for growth and ARS activity on solid medium, as shown

in Figure 1A. The growth of the *ars76* mutant in TAP medium was similar to that of wild-type 21 gr cells (Figure 1A, first panel on left, compare sectors *ars76* and 21 gr), but the mutant had essentially no ARS activity on TAP-S medium (S-depleted) (Figure 1A, third panel from the left, compare sectors *ars76* and 21 gr). This mutant exhibited no obvious change relative to wild-type 21 gr cells in the accumulation of extracellular phosphatase activity when the cells were grown on medium lacking P (Figure 1A, fourth panel from the left), suggesting that the mutant has the ability to export polypeptides when experiencing P deprivation (but see the section below on viability).

Initial analysis by adaptor ligation-mediated PCR indicated that the *AphVIII* insertion was in gene model Chlre2_kg.scaffold_11000188 (v3) (Pollock et al., 2005). Based on Augustus 5 predictions, gene model Chlre2_kg.scaffold_11000188 and three other contiguous gene models (given as 4 gene models in Chlre version 3 of the genome) were fused into a single model with the designation au5.g3281. Considering the size and multiple predicted functions associated with this single gene, it seemed likely that the current Augustus 5 model is not correct, and we therefore used the gene model information provided by Chlre version 3.0, which is shown in Figure 1B).

To generate the precise borders between the *Chlamydomonas* genomic sequence and the inserted *AphVIII* cassette, we walked along the genome from both the 3′ and 5′ ends of the cassette. These analyses showed that the insertion of the *AphVIII* cassette generated a 33,155-bp deletion in chromosome 12 that affected six predicted genes (Figure 1B, arrows indicate the borders of the deletion in the genomic DNA). Insertion of the *AphVIII* gene also deleted a 0.5-kb section of the cassette, leaving 448 bp of the *PSAD* promoter (upstream of the translation start site), which was enough to retain expression of the *AphVIII* gene.

Rescue of Mutant Phenotype

We introduced isolated DNA from BAC 36J16 (PTQ 13789) and BAC 8B3 (PTQ 2889), which contain combinations of the various genes that were deleted from the mutant genome of *ars76*. Both

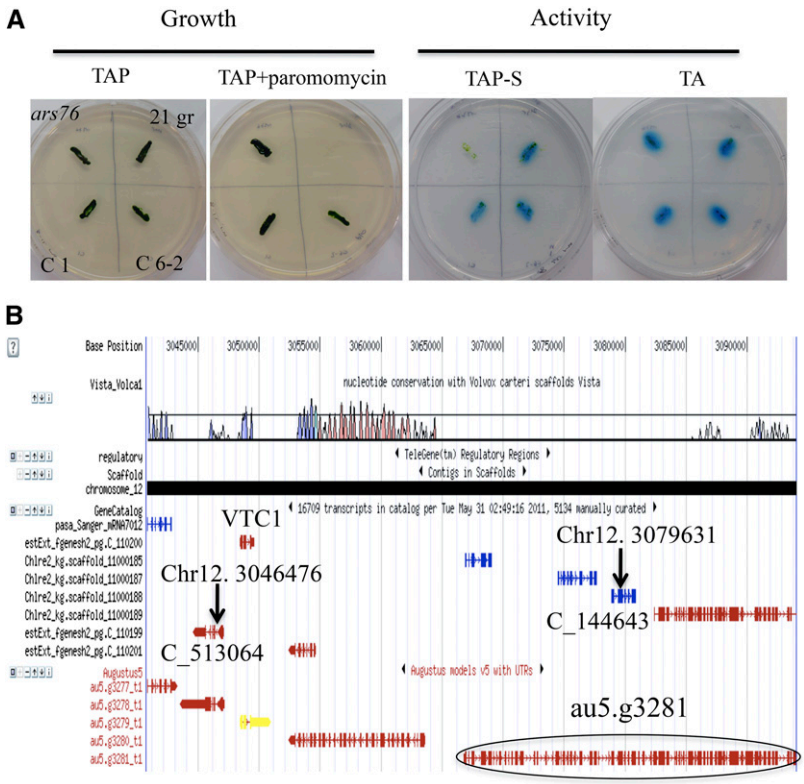

Figure 1. Characteristics of the *ars76* Mutant and Insertion Site in the Mutant Strain.

(A) Growth of 21 gr, *ars76*, and the rescued strains (C 1 and C 6-2, introduction of the *VTC1* gene). Growth was on TAP medium, TAP medium supplemented with paromomycin (TAP+paramomycin), and medium depleted of either S (TAP-S) or P (TA). ARS and phosphatase activities were evaluated on TAP-S and TA media, respectively.

(B) The genome browser showing the deletion of a 33,155-bp region of chromosome 12 that resulted from insertion of the paromomycin resistance cassette (*AphVIII*). The borders of the deleted region are indicated with arrows placed on the predicted transcripts (it extends from position 3046476, which is in intron 1 of gene model au5.g3278, protein ID 513064, to position 3079631, which is in exon 2 of gene model Chlre2_kg.scaffold_11000188, protein ID 144643 v3). Gene model au5.g3279 (Cre12g510250), VTC1 protein, which is indicated in the diagram, rescued the mutant phenotype.
Note: Augustus5 gene models may not be correct in this region. Gene model circled is a fusion of several gene models.

BACs were digested with *Xba*I, which restricts the *Chlamydomonas* genomic DNA in the BACs exclusively in intergenic regions, leaving all genes contained on the BAC insert intact. While no rescued strains were obtained when the mutant was transformed with BAC 8B3, we did achieve rescue when mutant cells were transformed with BAC 36J16; the rescued strain is designated C 6-2 in Figure 1A. Since BAC 36J16 contained three genes, we performed PCRs to determine which gene or genes were inserted in the genome of the C 6-2 complemented strain. This rescued strain only contained a newly introduced copy of the gene represented by model Cre12.g510250 (protein ID 513065 v5) (Figure 1B; Supplemental Figure 2A), which encodes a protein similar to a subunit of polyphosphate polymerase polypeptide designated VTC1 in *Saccharomyces cerevisiae*. We then transformed *ars76* specifically with the Cre12.g510250 or the *VTC1* gene expressed from its native promoter and obtained a number of rescued strains including C 1, C 2-1, and C 2-2 (C 2-1 and C 2-2 were obtained from the same electroporation cuvette). PCR analysis showed that these strains, like the initial rescued strain C 6-2, all had a wild-type copy of *VTC1* inserted in their genomes (Supplemental Figure 2A).

To further confirm that rescue of the mutant phenotype was a consequence of insertion of the *VTC1* sequence, we crossed strain C 6-2 with wild-type 21 gr and analyzed the paromomycin-resistant progeny to determine if ARS activity was linked to the presence of the introduced *VTC1* sequence. The presence of the newly introduced *VTC1* gene in the progeny was evaluated by PCR. In this cross, we would expect to generate some progeny that display an *ars*$^-$ phenotype because of random segregation of the chromosome that carries the introduced wild-type copy of *VTC1*, and chromosome 12, which has the endogenous *VTC1* gene eliminated as a consequence of insertion of the *AphVIII* cassette. Therefore, any paromomycin-resistant progeny exhibiting an *ars*$^-$ phenotype should not have the introduced wild-type copy of *VTC1*, whereas paromomycin-resistant progeny with an *ars*$^+$ phenotype should always have the introduced wild-type copy of *VTC1.* Phenotypic analyses of the progeny from three of the tetrads are shown in Supplemental Figure 2B (although more tetrads were analyzed). The analysis showed that *ars*$^+$ progeny all had a wild-type copy of *VTC1* and *ars*$^-$ progeny lacked the wild-type copy of *VTC1* (Supplemental Figure 2C). Two of the progeny (2 and 3) were not paromomycin resistant (these progeny would have at least one copy of the *VTC1* gene from wild-type 21 gr), while the other two were resistant to paromomycin (they would have the region with the deletion from *ars76* as well as the wild-type 21 gr introduced copy of *VTC1*). Progeny #1 and #3 of tetrad 2 had an *ars*$^-$ phenotype and were paromomycin resistant; these two progeny did not have a wild-type copy of *VTC1.* Progeny 2 and 4 from this tetrad had an *ars*$^+$ phenotype, were paromomycin sensitive and did have a wild-type copy of *VTC1* (derived from wild-type 21 gr) (Supplemental Figure 2C). In tetrad 3, progeny #4 had an *ars*$^-$ phenotype and did not have a wild-type copy of *VTC1*, while the other three products, which were *ars*$^+$, all had a wild-type copy of the gene (Supplemental Figure 2C). Analyses of addition progeny yielded the same phenotypic results. Hence, the *VTC1* gene rescues the phenotype (reestablishes the production of ARS in the mutant

A

```
CLUSTAL 2.1 multiple sequence alignment

C.reinhardtii       -MSLNNNNSTKMVTNYVFDKLYGTKQFTQGAELQLPRKVPMRVEPKSYFANERTFLSWMG
V.carteri           MSSILNNGNGKMASNYIFDKLYGTKQFTAGAELQLPRKVPMRVEPKSYFANERTFLSWMG
C.variabilis        --------MPTLQPSSLVDALWGTRTHTEGAQYQKPRKIPLRIEPKTYFANERTFLAWLG
S.cerevisiae        -----------MSSAPLLQRTPGKK-----------IALPTRVEPKVFFANERTFLSWLN
                              : .  :.:   *.:             :* *:*** :********:*:.

C.reinhardtii       MAITLGGVSSALVGFSGDS--EDTTEHLISKRTIDVITCIYSPLSILIMGYALFTYEWRS
V.carteri           MAITLGGVSSALVGFAGDADNEDTTDRLISKRTIDVITCIYSPLSILIMSYALFTYEWRS
C.variabilis        MATTLGTVSTAIAGFAVED-AEAKHKGGISQSTVELITLTLLPISIAMIAYALFTFYWRS
S.cerevisiae        FTVMLGGLGVGLLNFGDKIG--------------RVSAGLFTFVAMGTMIYALVTYHWRA
                    ::  ** :. .: .*. .                 : :     :::  : ***.*: **:

C.reinhardtii       KFMRTKQIGFFDDKVGPITVAVLVLLTLLSIFTIAVIDYLF----
V.carteri           KFMRTKQIGFFDDKIGPITVAGLVLMTLLVIFTVALIDYLF----
C.variabilis        EFIRRKQVGFFDDKLGPITLAVIVMISLTLIMLAAIKDLITNHK-
S.cerevisiae        AAIRRRGSGPYDDRLGPTLLCFFLLVAVIINFILRLKYNDANTKL
                      :* :  * :**::**  :. ::::::   :   :
```

B

Cre12.g510250.t1.2 (VTC1)

MSLNNNNSTKMVTNYVFDKLYGTKQFTQGAELQLPRKVPMRV**EPKSYFANERTFLS**
WMGMAITLGGVSSALVGFSGDSEDTTEHLISKRTIDVITCIYSPLSILIMGYALFTYEW
RSKFMRTKQIGFFDDKVGPITVAVLVLLTLLSIFTIAVIDYLF

Figure 2. Sequence and Structure of *Chlamydomonas* VTC1.

(A) Alignment of protein sequences of *Chlamydomonas* (*C. reinhardtii*) VCT1 with similar sequences from *Volvox carteri* (*V. carteri*), *Chlorella variabilis* (*C. variabilis*), and *S. cerevisiae*.

(B) Amino acid sequence and domain organization of VTC1. The amino acids given in bold represent the VTC domain and the underlined amino acids represent transmembrane domains.

strain), and the results confirm that the product of *VTC1* appears to function in the acclimation of *Chlamydomonas* to S deprivation.

Structure and Function of VTC1

A BLAST search of the NCBI database using the VTC1 sequence identified close homologs of VTC1 (Figure 2A**)**. The regions of similarity are conserved among other species and include a VTC domain and transmembrane domains (Figure 2B). This domain architecture of *Chlamydomonas* VTC1 is very similar to that of *S. cerevisiae* Vtc1p, although the three algal sequences shown all have two insertions of between 11 and 14 amino acids relative to the *S. cerevisiae* sequence.

S. cerevisiae Vtc1p is present in a complex that is involved in acidocalcisome membrane fusion events and polyphosphate synthesis (Ogawa et al., 2000; Uttenweiler et al., 2007; Hothorn et al., 2009), while *S. cerevisiae* Vtc4p is a polyphosphate polymerase (Hothorn et al., 2009). Other proteins associated with various vacuole types have been analyzed through mutational studies and shown to be involved in contractile vacuole function, autophagy, cytokinesis, and lysosomal inactivation of Parainfluenza virus (Komsic-Buchmann et al., 2012; Ding et al., 2014; Tenenboim et al., 2014). The Vtc proteins of *S. cerevisiae* appear to assemble into a complex whose formation requires all of the polypeptide subunits of the complex. Therefore, it is likely that no VTC complex forms and that no polyphosphate accumulates in the absence of *Chlamydomonas* VTC1. To probe the impact of the lesion on cellular structure and polyphosphate accumulation, we performed transmission electron microscopy (TEM) analysis of wild-type 21 gr, *ars76*, and C 6-2. Under nutrient-replete conditions, we were unable to detect any structural abnormalities in the *ars76* mutant, e.g., the nucleus and chloroplast appeared similar in mutant and wild-type 21 gr cells (Figure 3A). However, after 48 h of S starvation, we observed many fewer electron dense acidocalcisomes (vacuoles containing polyphosphate granules) in the *ars76* cytoplasm relative to wild-type 21 gr and C 6-2, with most of the mutant cells showing less internal structure, essentially no clearly identifiable vacuoles and more membrane deformations than wild-type 21 gr (Figure 3B). The *ars76* mutant cells also lack vacuoles and polyphosphate bodies (Figure 4). Interestingly, as also observed by Komine et al. (2000), we noted Golgi stacks positioned near the acidocalcisome in wild-type 21 gr, suggesting a possible function for these organelles in protein trafficking (Figure 5; Supplemental Figure 3). We observed this in the C 6-2 rescued strain (Figure 4A); however, since there are no identifiable acidocalcisomes in the *ars76* mutant and most cells already showed deformations, this phenomenon could not be observed in *ars76* (Figure 4B).

We also performed 4′,6-diamidino-2-phenylindole (DAPI) staining of wild-type 21 gr and *ars76* cells to specifically evaluate the presence of polyphosphate and acidocalcisomes in late log phase cultures (6×10^6 cells/mL). We detected a strong fluorescence signal from wild-type 21 gr cells (Figure 6; Supplemental Figure 4); however, the level of DAPI fluorescence was very low in the *ars76* mutant (background levels), again confirming that either no or little accumulation of polyphosphate occurred in the mutant (Figure 6; Supplemental Figure 4).

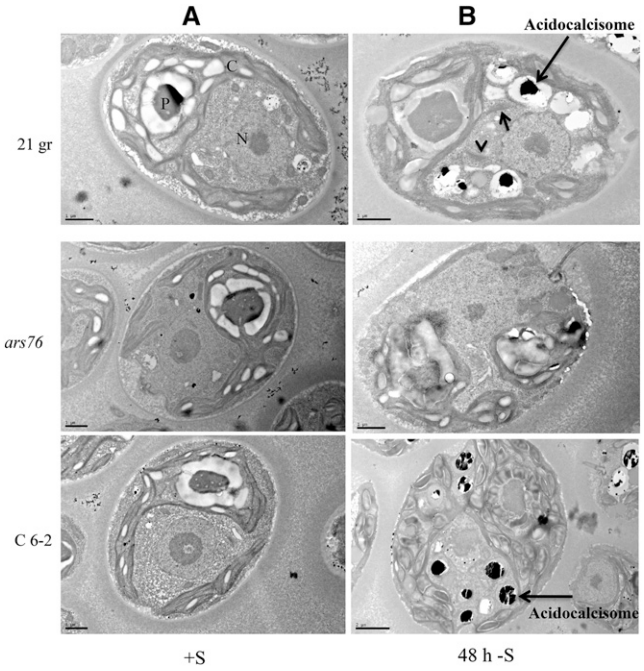

Figure 3. TEM Images of *Chlamydomonas* Grown under Nutrient Replete and S Deprivation Conditions.

(A) Wild-type 21 gr, *ars76*, and C 6-2 cells grown in TAP medium.
(B) Wild-type 21 gr, *ars76*, and C 6-2 cells that were S-starved for 48 h. Notice the loss of the majority of vacuoles in *ars76.* Arrow and arrowhead point to Golgi stacks. See Figure 5 for higher magnification of region marked with the arrow. N, nucleus; C, chloroplast; P, pyrenoid. Acidicalcisomes that form under –S conditions are marked with arrows in 21 gr and C 6-2 cells. Bars = 1 μm, except for C 6-2 48 h –S, which is 2 μm.

Expression of *VTC1*

We quantified levels of the transcript encoding VTC1 in wild-type 21 gr, *ars76*, and the rescued C 6-2 strain. The mRNA was isolated from cells grown in TAP (S-replete) or maintained for different times (30 min, 4 h, 6 h, and 24 h) on medium without S (S-depleted). Reverse transcription and quantitative PCR (RT-qPCR) showed that the *Chlamydomonas VTC1* transcript levels were similar in S-replete and S-depleted (6 h) wild-type 21 gr cells (Figure 7A). The mRNA was not detected in the *ars76* mutant strain, as expected, while the level of transcript in the rescued C 6-2 strain was similar to that of wild-type 21 gr cells (Figure 7A). *VTC1* mRNA from *ars76* and C 6-2 were also examined using RT-PCR at various times after cultures were exposed to S deprivation; *VCT1* mRNA was never detected in mutant cells (although the control transcript, *CBLP* was present), while for the rescued strain, C 6-2, it remained at similar levels at all times after the imposition of S deprivation (30 min, 4 h, and 24 h) (Figure 7B). Furthermore, RNA-seq data also showed that the level of *VTC1* mRNA in wild-type 21 gr cells remained approximately constant during S deprivation. Also, the *ars11* mutant (also designated *snrk2.1* because it does not make the S deprivation protein kinase SNRK2.1) (Gonzalez-Ballester et al., 2008), which is defective for a key regulatory element of the S deprivation response, has

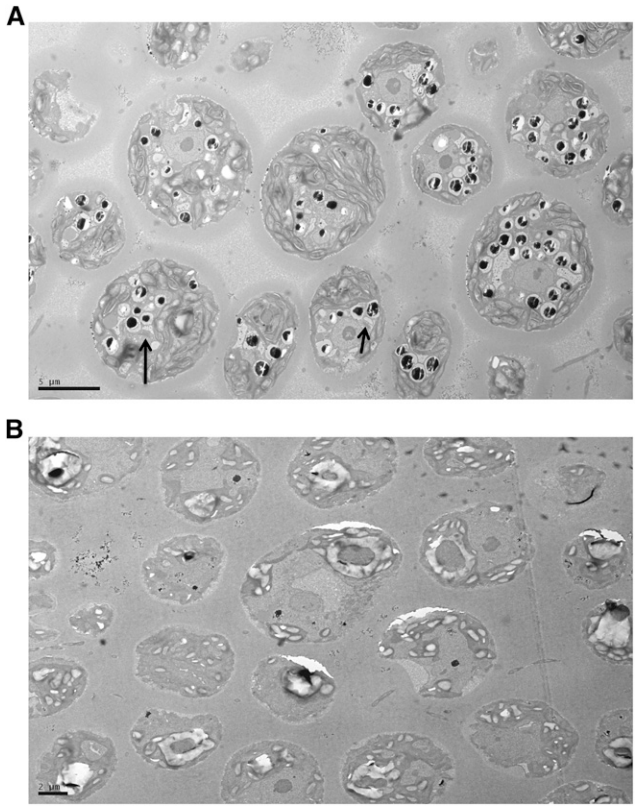

Figure 4. TEM Showing Acidocalcisomes in C 6-2 under –S Conditions.

Acidocalcisomes in C 6-2 strain **(A)** and the *ars76* mutant **(B)**. Golgi stacks near vacuoles are marked with arrows (in **[A]**). Note, *ars76* does not appear to develop acidocalcisomes and exhibits structural deformations. Bars = 5 μm in **(A)** and 2 μm in **(B)**.

normal levels of *VTC1* mRNA (Supplemental Figure 5); this latter result indicates that *VTC1* is not under the control of SNRK2.1.

Expression of S-Deprivation-Responsive Genes in the *ars76* Mutant

VTC proteins have been shown to be involved in vacuolar membrane fusion, polyphosphate synthesis, and microautophagy in *S. cerevisiae* (Cohen et al., 1999; Ogawa et al., 2000; Müller et al., 2002; Uttenweiler et al., 2007; Hothorn et al., 2009). Strains of *S. cerevisiae* with lesions in *Vtc1p* exhibit decreased levels of polyphosphate and defects in vacuolar membrane fusion. The *ars76* mutant of *Chlamydomonas* exhibited normal phosphatase activity under P deprivation conditions, suggesting that some aspects of the P deprivation responses are normal in this strain (Figure 1A, rightmost panel), even though the mutant is unable to properly acclimate to S deficiency or to accumulate acidocalcisomes.

To further characterize S deprivation regulation of genes in the *ars76* mutant, we assayed for accumulation of various known S-responsive transcripts. mRNAs encoding ARS1 and ARS2 increased by ~1000-fold in wild-type 21 gr, but there was essentially no and little increase in the *ARS1* and *ARS2* transcripts, respectively, in the *ars76* mutant (Figure 8A). The levels of mRNAs encoding the extracellular proteins (ECPs; putative cell wall proteins synthesized under S deprivation conditions) under S-replete conditions were nearly undetectable in wild-type 21 gr (except for *ECP56*), but increased between 100-fold (*ECP56*) and >1000-fold (*ECP61*, *ECP76*, and *ECP88*) following S deprivation. In contrast, the *ECP56*, *ECP76*, and *ECP88* transcripts were essentially undetectable in the *ars76* mutant in either S-replete or S-depleted conditions, while there was some S deprivation-elicited increase in *ECP61* transcript accumulation, although not to nearly the same level as in wild-type 21 gr cells. Additionally, *ars76* exhibited lower levels of *HAP2* mRNA accumulation than that of wild-type 21 gr cells upon S deprivation (little induction occurred in the mutant strain) (Figure 8A). The levels of ARS, ECP, and HAP2 transcripts are all restored to near wild-type levels in the C 6-2 rescued strain (the levels might be slightly lower for some ECP transcripts). Furthermore, immunoblot data shows that the level of ARS protein is generally in accord with the transcript data; the protein could not be detected under plus S conditions and accumulated to a very low level in the *ars76* mutant under S deprivation conditions. It is not clear whether the protein that does accumulate in the mutant is intracellular or extracellular. This phenotype is rescued in the C 6-2 rescued strain, which accumulated similar levels of the ARS protein as that of wild-type 21 gr cells (Figure 8B).

The levels of transcript from genes encoding the inducible high-affinity sulfate transporters (*SLT1*, *SLT2*, and *SULTR2*) following 24 h of S deprivation were generally somewhat lower (from ~5- to 10-fold) in *ars76* than in wild-type 21 gr cells (Figure 9A), although the impact of the lesion on the levels of these transcripts wasn't nearly as dramatic as that observed for those of the extracellular *ARS*s and *ECP*s. The mutant strain also showed a relatively normal decline in the level of mRNA for the low affinity sulfate transporter, SULTR1, during S deprivation. Congruent with the RT-qPCR data, levels of transporter proteins were also significantly lower in *ars76* than in wild-type 21 gr

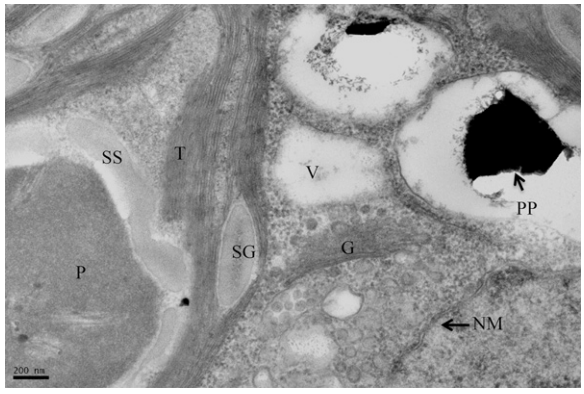

Figure 5. High Magnification Image Showing Disposition of Vacuole and Golgi.

Region marked with an arrow in Figure 3B but at 8000× magnification, showing vesicles potentially leaving Golgi stocks and fusing with vacuoles as described by Komine et al. (2000). The positions of the vacuoles are interior to the apical regions of chloroplast (see Figure 3B). P, pyrenoid; SS, starch sheet around pyrenoids; T, thylakoid membranes; SG, starch granules in thylakoid membranes; V, vacuole; G, Golgi; NM, nuclear membrane; PP, polyphosphate in vacuoles; acidocalcisomes. Bar = 200 nm.

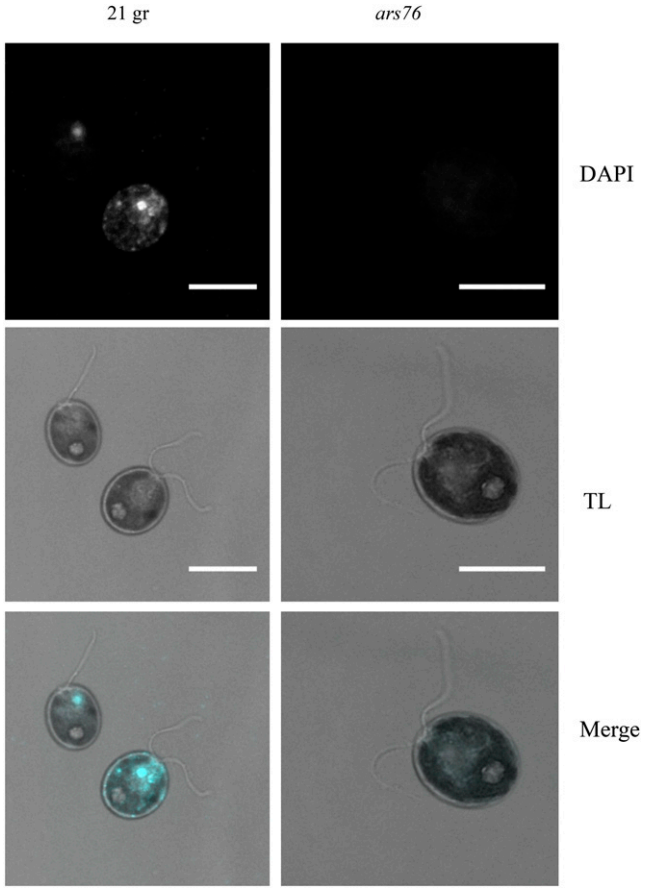

Figure 6. Staining Polyphosphate with DAPI.

Wild-type 21 gr and *ars76* cells were grown in TAP medium to ~6 × 10^6 cells/mL and incubated with DAPI. DAPI was excited at 405 nm and emission spectrum of 532 to 632 nm was collected using a Leica SP5 scanning confocal microscope. DAPI, DAPI fluorescent images in gray scale; TL, transmitted light images; merge, overlay of fluorescent and transmitted light images shown in blue. Bar = 10 μm.

cells, with the greatest impact on the level of the SULTR2 protein. Essentially normal levels of the transporters were restored in the C 6-2 strain (Figure 9B).

ARS73a was previously shown to be involved in the regulation of a subset of S-responsive genes (Aksoy et al., 2013), while SNRK2.1 is a major regulator essential for many S deficiency responses (Gonzalez-Ballester et al., 2008). The mRNAs from both of these genes were impacted to some extent in the *ars76* mutant relative to wild-type 21 gr (Figure 10; the levels are ~5-fold lower then wild-type 21 gr). RNA-seq data shows that the *snrk2.1* mutant is not able to downregulate the *SULTR1* mRNA, suggesting that *SNRK2.1* controls the decline of *SULTR1* mRNA during S deprivation (González-Ballester et al., 2010). Since the regulation of *SULTR1* mRNA appears to be normal in the *ars76* mutant, it is likely that the SNRK2.1 protein in *ars76* is functioning as it does in wild-type cells. The increase in the level of the *LHCBM9* transcript also appeared normal in *ars76* mutant, while that of *SBDP* was only slightly reduced (Figure 10). Interestingly, rescue of ARS73a and SNRK2.1 transcript levels was not complete in C 6-2, suggesting that the decrease in transcription of these genes might not be related to VTC1 but might be a consequence of the large deletion in the locus. Together, these results suggest that the cells can still sense S deprivation but that the responses are not as robust as in the wild-type strain (possibly because of reduced fitness under stress conditions), with the greatest impact on the production of extracellular proteins (both at the level of transcript and protein, at least for the ARS and potentially most ECPs, although we do not have antibodies to quantify levels of ECPs). The less extreme reduction in levels of some transcripts in mutant cells (e.g., SBDP) might reflect the more general inability of the cells to fully acclimate to the deprivation conditions, which might dampen the extent of the response.

Viability of the *ars76* Strain Following S or P Deprivation

We tested the effect of the *ars76* lesion on viability/survival of cells during S, P, or N deprivation. To determine the proportion of viable cells after exposing cultures to various times of nutrient deprivation, we spotted equal amounts of culture volume onto

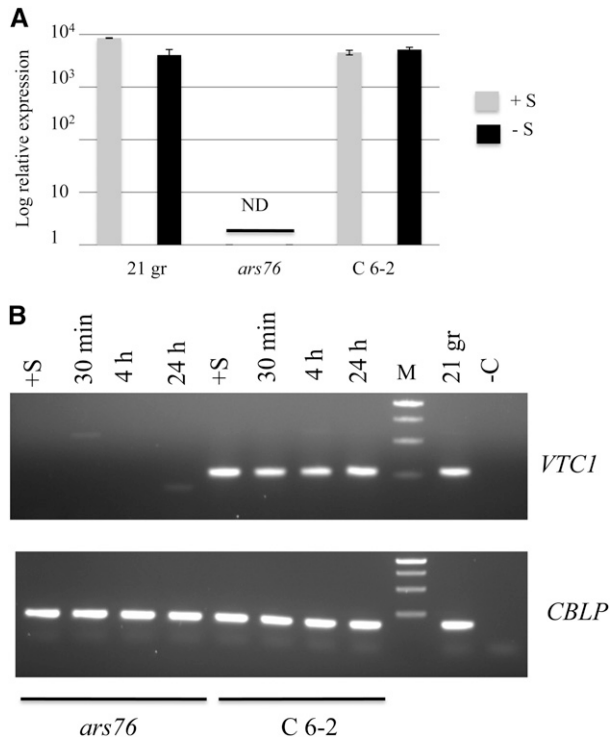

Figure 7. Expression of *VTC1*.

(A) RT-qPCR analysis of expression of *VTC1* in wild-type 21 gr, *ars76*, and the C 6-2 rescued strain.

(B) RT-PCR showing expression of *VTC1* in the mutant and rescued strains (C 6-2) at various times following the initiation of S deprivation. RNA samples were collected at the indicated times after placing the cells in S-depleted medium. RT-PCR of the *CBLP* transcript was used as an internal control. -C represents the no RT negative control and ND is nondetected. Error bars represent standard deviations of experiments based on two biological replicates, each with three technical replicates.

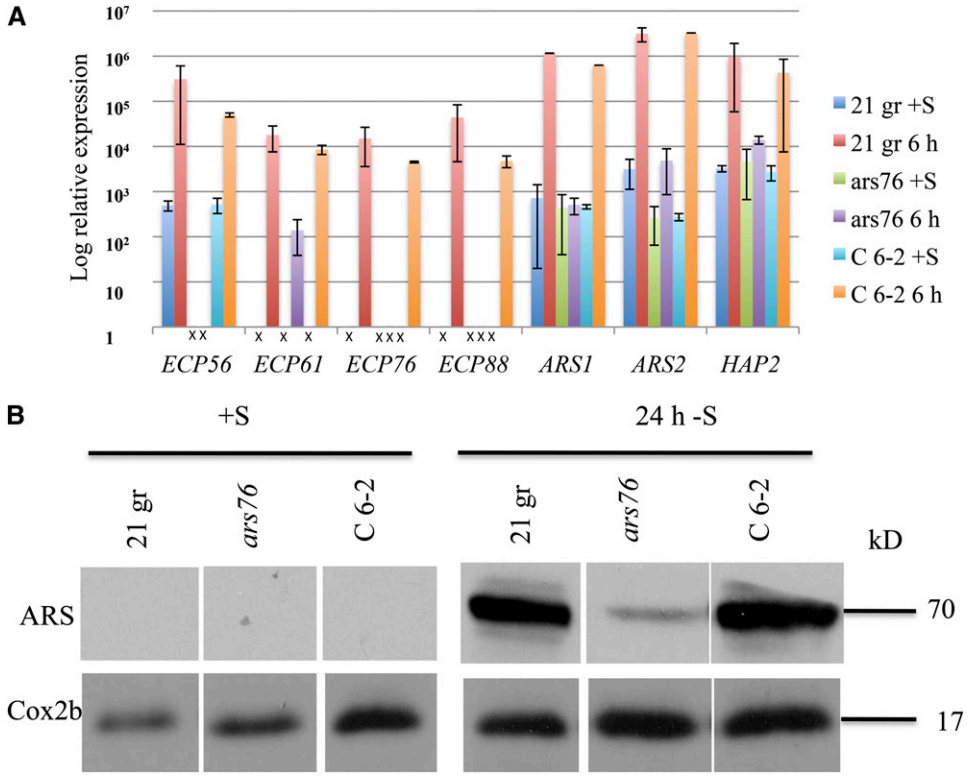

Figure 8. Transcript and Protein Levels of Genes Encoding Various Extracellular Proteins.

(A) RT-qPCR to determine relative mRNA levels from the *ARS1*, *ARS2*, *ECP56*, *ECP61*, *ECP76*, *ECP88*, and *HAP2* genes in wild-type 21 gr, *ars76*, and C 6-2 under both S-sufficient and S-depleted conditions. "X" indicates that no signal was detected.

(B) Immunoblots showing levels of ARS proteins in wild-type 21 gr, *ars76*, and C 6-2. The COX2b protein was used as a loading control. Molecular masses of the proteins are shown to the right of the gel image. The data in **(B)** are all from a single immunoblot; all times of exposure for a given antibody are the same. Error bars represent standard deviations of experiments based on three biological replicates, each with three technical replicates.

TAP medium before and at different times after the cells were exposed to either S, P, or N deprivation. The *ars76* mutant appeared to die somewhat more rapidly than wild-type 21 gr during S deprivation (Figure 11A); mutant cells also bleached more rapidly (Figures 11A and 11B). The bleaching and death of the *ars76* cells were similar to that of the *ars11* (*snrk2.1*) mutant. Interestingly, the lesion also appeared to affect the growth of cells during P deprivation; P-deprived mutant cells attain lower densities and/or have less chlorophyll than parental cells. The effect of P starvation is more obvious for *ars76* after 51 d of P starvation (Figure 11C). These results demonstrate that VTC1 is necessary for the proper acclimation of *Chlamydomonas* to both S and P deficiency, although the impact on S deprivation appears to be much more pronounced.

Quantitative growth studies showed that the *ars76* mutant exhibited a small, but not statistically significant, overall decrease in the rate of growth relative to wild-type 21 gr under nutrient-replete conditions (Figures 12A and 12B) . Furthermore, the rescued strain (C 6-2) did not reach the same density as the wild-type strain; it had 25 to 30% fewer cells/mL based on cell number (Figure 12A). However, the chlorophyll amount per cell was also somewhat different in *ars76* than in wild-type 21 gr cells, although it did have the same amount of chlorophyll per culture volume (somewhat more chlorophyll per cell for the mutant and the rescued strain relative to wild-type 21 gr) **(**Figure 12B). The chlorophyll *a/b* ratio was not significantly different in the mutant compared with wild-type 21 gr, although the rescued strain (C 6-2) did have a slightly lower chlorophyll *a/b* ratio **(**Figure 12C), which suggests that there is a little more chlorophyll associated with light harvesting antennae relative to reaction centers in the C 6-2 strain under the growth conditions used.

Overall, these results suggest that the *ars76* mutant is severely diminished in its ability to withstand S and P deprivation. Furthermore, although the mutant was readily crossed and therefore capable of forming gametes when placed in medium lacking N, the N-deprived cells did not accumulate detectable levels of L amino acid oxidase 1 (LAO1) (Supplemental Figure 6A). Interestingly, we did observe an initial increase in the *LAO1* mRNA in the *ars76* mutant upon 2 h of N depletion, but this accumulation rapidly declined and was 10-fold lower after 2 d; the level of transcript for wild-type 21 gr and C 6-2 cells remained high after 2 d of N starvation. The transcript encoding the NIT1 protein, a cytosolic nitrate reductase, remained high over the 2 d of these experiments (Supplemental Figure 6B). Viability of *ars76* was also affected when cells were deprived of N; mutant cells died more rapidly than wild-type 21 gr cells

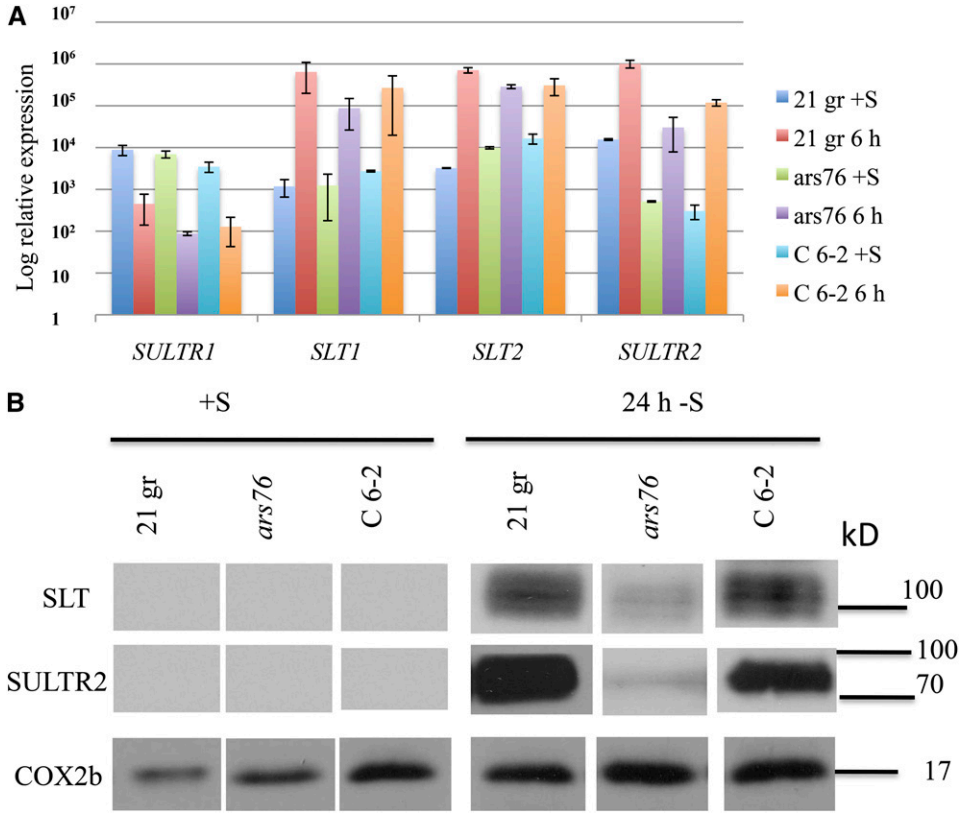

Figure 9. Analysis of Sulfate Transporter Transcripts and Proteins.

(A) RT-qPCR analysis was performed to determine relative levels of the mRNA encoding the low affinity (SULTR1) and high affinity (SLT1, SLT2, and SULTR2) sulfate transporters.

(B) Immunoblot analysis to determine levels of sulfate transporter proteins. Error bars represent standard deviations of experiments bases on two biological replicates, each with three technical replicates.

(Supplemental Figure 7A) and also had reduced chlorophyll levels (Supplemental Figure 7B). These results again suggest that *ars76* has a more general defect in its ability to acclimate to nutrient deficiency (and perhaps other stress conditions) and that the primary defect in the mutant most likely involves the proper targeting of proteins to their site of function in the periplasmic space, and perhaps also in the plasma membrane.

Overall, the transcript data show that the *ars76* mutant does not accumulate mRNAs encoding proteins that require secretory processes for their biogenesis during S deprivation (and also during N deprivation) and especially those encoding the extracellular proteins ARS1, ARS2, the various ECPs, and HAP2, with less of an effect on the integral membrane sulfate transporters (Figures 8A and 9A). Furthermore, evaluation of protein levels demonstrates that the decreased transcript levels are paralleled by decreased protein levels for at least ARS and the sulfate transporters (Figures 8B and 9B). For LAO1, we detected significant levels of the transcript, especially very soon after exposing cells to N deprivation, but were unable to detect the protein. Transcripts encoding intracellular proteins that are not secreted by the cells during acclimation, including *CBLP*, *LHCBM9*, and *NIT1* are not significantly impacted in the *ars76* strain (Figures 7 and 10; Supplemental Figure 6).

DISCUSSION

Based on a forward genetic screen for identifying strains unable to accumulate ARS activity (Pollock et al., 2005) during S deprivation, we isolated the *Chlamydomonas* mutant *ars76*. This mutant cannot properly acclimate to S deprivation, accumulating essentially no ARS activity and little ARS protein when depleted for S. Other indications that the mutant is unable to properly acclimate to S deprivation are an inability of the cells to accumulate transcripts encoding ARS, the ECPs, and HAP2 (Figure 8A), all of which code for proteins localized to the extracellular space. While transcripts and proteins encoding the sulfate transporters were also reduced in the mutant (Figure 9), other S-responsive transcripts (e.g., encoding LHCBM9) (González-Ballester et al., 2010) showed a relatively normal S deprivation-elicited increase in accumulation. These results suggest that the *ars76* lesion strongly impacts accumulation of transcripts and activities associated with extracellular proteins and to a lesser extent, membrane-associated proteins. We also noted a number of responses suggesting that the mutant cells experience more severe stress than wild-type 21 gr when deprived of S. Such responses, which are more rapid or extreme in the mutant than wild-type 21 gr or the C 6-2 rescued strain, include (1) induction of genes associated with autophagy

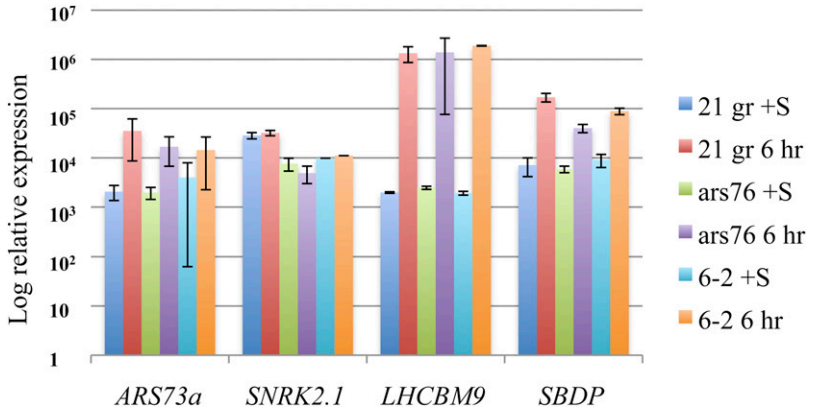

Figure 10. Relative mRNA Levels from Genes Associated with S Deprivation as Determined by RT-qPCR.

The mRNA levels of *ARS73a*, which encodes a protein involved in transcription of a subset of S-responsive genes, *SNRK2*.1, which encodes a serine-threonine protein kinase that impacts most aspects of the S-deprivation responses, *LHCBM9*, which encodes a light harvesting protein, and *SBDP*, which encodes a selenobinding protein, were quantified both before and 6 h following the removal of S from the medium. Transcript analysis was performed with RNA extracted from wild-type 21 gr, *ars76*, and the C 6-2 rescued strain. Error bars represent standard deviations of experiments based on two biological replicates, each experiment with three technical replicates.

(Supplemental Figure 8; relatively small impact), which are elicited in *Chlamydomonas* under various stress conditions (Pérez-Pérez et al., 2010); (2) loss of chlorophyll or bleaching; and (3) a decline in cell viability. Indeed, mutant cells die significantly more rapidly during N, P, or S deprivation than wild-type 21 gr, a difference observed as early as 2 to 3 d following the initiation of S depletion. The impact of the lesion is significantly more pronounced under S deficiency than P deficiency (Figure 11).

The deleted gene responsible for the *ars*$^-$ phenotype in *ars76* encodes a putative VTC1 (similar to Vtc1p of *S. cerevisiae*). Vtc proteins of *S. cerevisiae* assemble into a complex (containing subunits Vtc1p-Vtc4p) that is involved in several membrane-associated processes including the sorting of integral membrane ATPases, endocytosis, vacuolar-membrane fusion, budding of autophagic vesicles into the lumen of vacuoles, and trafficking between the endoplasmic reticulum and Golgi (Cohen et al., 1999; Ogawa et al., 2000; Müller et al., 2002, 2003; Uttenweiler et al., 2007). Deprivation of wild-type 21 gr cells for S triggers the budding of vesicles from the Golgi stacks that appear to be directed toward vacuoles, with some vesicles that might be in the process of fusing with the vacuole, which might contain polyphosphate and be considered an acidocalcisomes (Figure 5; Supplemental Figure 3). Acidocalcisomes may be interior to the apical region of the chloroplast (Figure 3B) and positioned to receive proteins en route to their site of function, which in the case for ARS, ECP, and LAO would be the periplasmic space. There are no distinct cytosolic vacuoles/acidocalcisomes in the *ars76* mutant (Figures 3B and 4B), which suggests that elimination of VTC1 of *Chlamydomonas* causes a marked decrease in observable acidocalcisomes. This, in turn, might result in an inability to deliver S- and N-responsive periplasmic proteins to their site of function. Interestingly, in *S. cerevisiae*, the Vtc complex was shown to be involved in polyphosphate synthesis (Ogawa et al., 2000; Hothorn et al., 2009); in addition to being localized to the acidocalcisome, polyphosphate is also found in the cell wall and potentially functions in retaining proteins in periplasmic space (Freimoser et al., 2006; Werner et al., 2007). The processes of membrane fusion/budding and polyphosphate synthesis might have overlapping functions that are critical for maintaining proper acidocalcisome function; polyphosphate levels within acidocalcisomes might influence bioenergetic processes and membrane dynamics and might be considered a signature associated with the development of the acidocalcisomes from a vacuole, which might have more generalized and/or different functions. The function of the Vtc complex in acidocalcisome membrane fusions may involve a role in SNARE priming, V_0 trans-complex formation (Vtc1p and Vtc4p), and late stages of membrane fusion and possibly the development of the fusion pore opening (Vtc3p) (Müller et al., 2002). Experiments with *S. cerevisiae* clearly show that Vtc proteins impact acidocalcisome membrane fusion events by influencing V-ATPase conformation and stability. The Vtc proteins have also been implicated in proton uptake as a consequence of conformational changes in the V-ATPase (Cohen et al., 1999; Müller et al., 2002).

If the *ars76* mutant exhibits aberrations in acidocalcisome function and trafficking of vesicles both within the cell and to the extracellular space during S deprivation, we might expect to observe atypical membrane morphologies under both nutrient-replete and deprivation conditions. The cellular architecture of the *ars76* mutant appears to be similar to that of wild-type 21 gr under nutrient-replete conditions (Figure 3A; both cell types have few putative acidocalcisomes in the cytosol); however, mutant cells exhibited reduced vacuolarization with significant membrane deformations relative to wild-type 21 gr and the C 6-2 rescued cells after exposure to S-limited growth conditions (Figures 3B and 4B). Furthermore, the *ars76* mutant had no observable polyphosphate as assayed by DAPI staining (Figure 6; Supplemental Figure 4). Therefore, the various *ars76* phenotypes coupled with the reported functions of *S. cerevisiae* Vtc1p/Vtc complex in membrane trafficking/fusion/vacuolar uptake suggests that VTC1 of *Chlamydomonas* is involved in protein trafficking/maturation either directly or indirectly, that it is critical for the acclimation of cells to S deprivation (and perhaps also

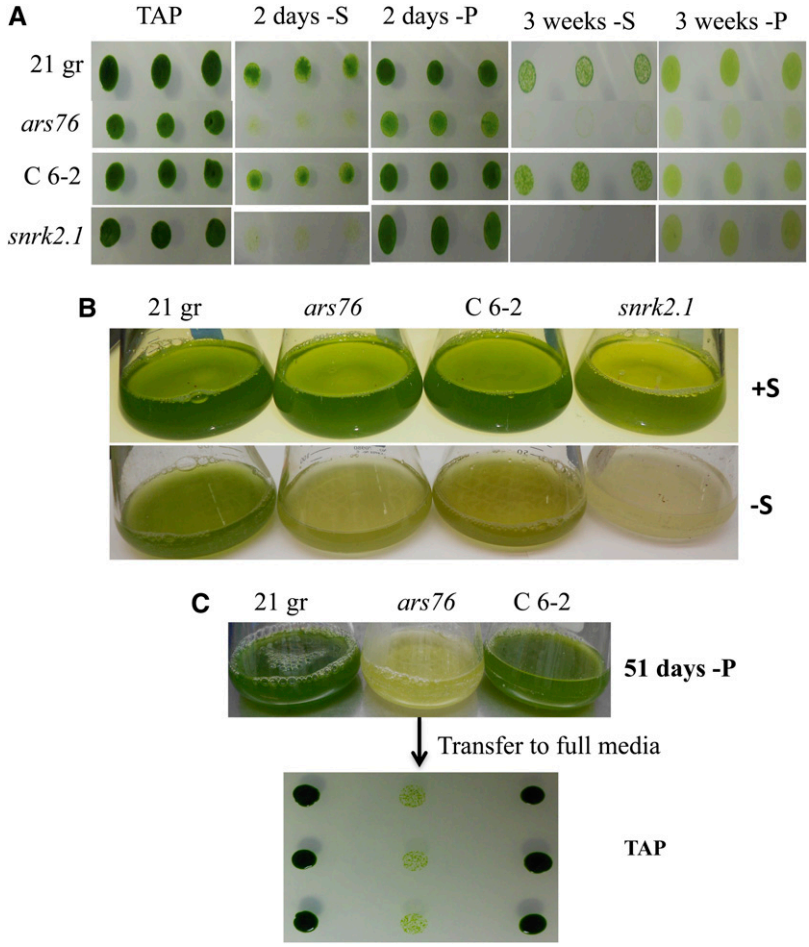

Figure 11. Impact of *ars76* Lesion on Growth and Bleaching during S and P Deprivation.

(A) S and P deprivation of the wild-type 21 gr, *ars76*, *snrk2.1*, and the *ars76* complemented strain C 6-2. Equal amounts of cultures were spotted onto TAP solid medium before and after nutrient deprivation (for 2 d and 3 weeks).
(B) Wild-type 21 gr, mutant, and rescued cultures were grown in liquid medium with and without S for 3 weeks, as indicated in the figure.
(C) Cultures after 51 d under –P conditions and recovery on TAP medium after 51 d of P starvation.

N and P deprivation), and that it is more specific to S than P deprivation conditions. Part of the complexity of the aberrant biochemical responses observed in the mutant may reflect the inability of the cells to efficiently recycle amino acids and other macromolecules when they are deprived of S because of an inability to establish vacuolar/acidocalcisome compartments and associated fusion functions. For example, recycling macromolecules in the vacuole or developing acidocalcisome may be critical for acquiring building blocks needed for the synthesis of new sets of proteins, lipids, and other compounds as the cells acclimate to new conditions. However, it is also possible that as the cells experience nutrient limitation the forming vacuoles might, as suggested by Komine et al. (2000), be directly involved in packaging material for transport to various cellular locations, including the periplasmic space.

As implied in the discussion above, there is specificity to the role of VTC1 in protein trafficking in *Chlamydomonas*. Mutant cells appear minimally affected during nutrient-replete growth, and unlike wild-type 21 gr cells, *ars76* does not accumulate extracellular ARS (Figures 1 and 8) or LAO1 (Supplemental Figure 6) when deprived of S and N, respectively, but does accumulate extracellular phosphatase activity when deprived of P (Figure 1). While the recycling and synthesis of specific sets of proteins may be controlled by impairment of vacuolar function in *ars76*, it is more likely that the mutant phenotype reflects aberrations in trafficking and that there is more than one mode for routing proteins to the extracellular space; localization of ARS and LAO1 to the periplasmic space requires the VTC complex, while localization of the extracellular PHOX protein (Quisel et al., 1996) is VTC independent (or another protein can substitute for VTC1 during P deprivation).

In *S. cerevisiae*, the Vtc4p subunit of the VTC complex has polyphosphate kinase activity, which is responsible for accumulation of polyphosphate granules in acidocalcisomes. We identified *Chlamydomonas* genes encoding other putative VTC proteins, including VTC4 (Supplemental Figure 9). The *ars76* mutant

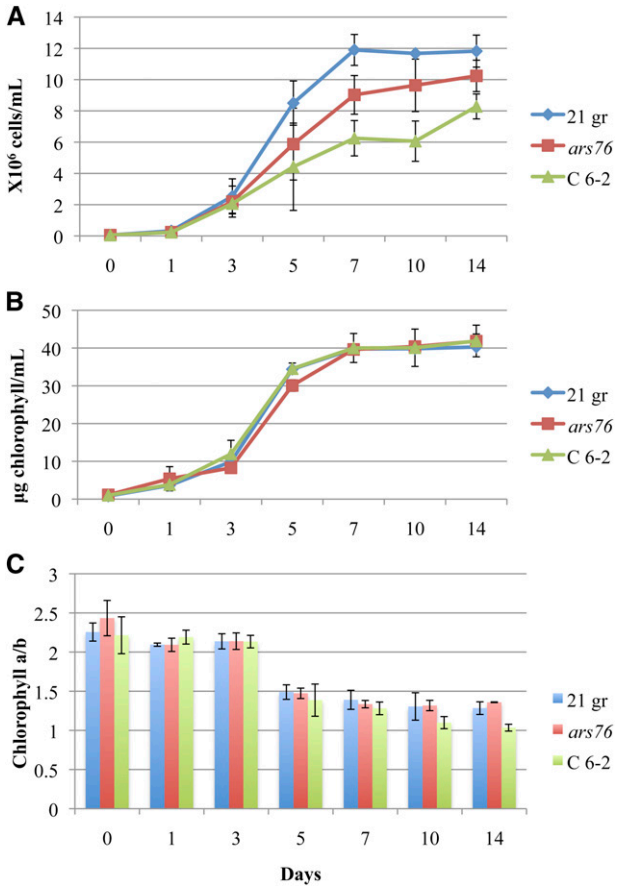

Figure 12. Growth in TAP Medium.

Cultures were started with an equal amount of cells (5 × 10^4 cells/mL). Growth based on cell number **(A)**, growth based on total chlorophyll content **(B)**, and the chlorophyll *a*/*b* ratios determined at the times indicated (from 1 to 18 d) following the initiation of growth in moderate light **(C)** (40 μmol photons m^{-2} s^{-1}). The data shown are the results of two biological replicates, each containing three technical replicates; error bars represent the SD.

[See online article for color version of this figure.]

appears to be defective for the synthesis of polyphosphate and while acidocalcisomes were shown to accumulate in wild-type 21 gr cells during S deprivation (based on DAPI staining and TEM), no such vacuoles were observed in *ars76* (Figures 3B, 4B, and 6; Supplemental Figure 4). Polyphosphate has been found to serve as a counterion for both inorganic (e.g., heavy metals) and organic cations and has also been implicated in regulatory processes (Moreno and Docampo, 2013). Furthermore, we cannot exclude the possibility that the inability of the mutant to accumulate polyphosphate creates a problem in the trafficking of proteins during N and S deprivation. During P deprivation, there would be no accumulation of polyphosphate in vacuoles of wild-type 21 gr cells since deprived cells would use all available P to facilitate the acclimation process. Therefore, the recycling of polyphosphate would likely not be involved in the localization of extracellular proteins during P deprivation.

In addition to the loss of ARS activity in *ars76*, this strain fails to accumulate ARS transcripts in response to S deprivation. A similar inability to accumulate transcripts encoding other S-responsive periplasmic proteins was also observed (e.g., transcripts for ECPs and HAP2). This finding suggests that the mutant can no longer activate genes encoding these periplasmic proteins when the cells are deprived of S. Interestingly, although no LAO1 protein was detected in the *ars76* mutant during N deprivation, the transcript accumulated to some extent during the early stages of N deprivation but then showed a significant decline that was not observed in either wild-type 21 gr cells or C 6-2 (Supplemental Figure 6). Furthermore, accumulation of inducible alkaline phosphatase activity (*PHOX*) was not significantly impacted in the mutant. The phenotypes of the *Chlamydomonas ars76* mutant may reflect the various roles of the VTC complex as defined for *S. cerevisiae*. We propose that the primary lesion in *ars76* affects amino acid recycling (recycling of proteins in the vacuole/lysosome) and that the secretion and localization of several nascent polypeptides to the periplasmic space (and perhaps also the plasma membrane) during S and N deprivation reflects the role of the VTC complex in vacuole function and fusion of membrane vesicles. This also prevents the formation of acidocalcisomes, which occurs during later stages of nutrient deprivation. Furthermore, the inability to complete the biogenesis process creates a bottleneck in the system that activates a checkpoint/feedback control that suppresses gene activity. However, it is also possible that elimination of *VTC1* could have a direct impact on levels of transcripts encoding ARS, other secretory proteins (including LAO1) and the sulfate transporters. We favor the first explanation, based on the defined function of the VTC complex in *S. cerevisiae* and the finding that the N deprivation-inducible, extracellular LAO1 does not accumulate in *ars76* when the cells are starved for N, while the *LAO1* transcript is still induced and only declines after 1 to 2 d of N deprivation. The pleiotropic nature of the mutation is further supported by the finding that during N, P, or S deprivation the *ars76* strain dies more rapidly than wild-type 21 gr cells, even though extracellular PHOX activity accumulates to approximately the same level (activity) as in wild-type 21 gr cells during P deprivation. This finding also raises the possibility that there are multiple pathways by which a protein can be exported into the periplasmic space of *Chlamydomonas* cells, including VTC sensitive and insensitive pathways.

As discussed, the VTC complex is required for polyphosphate synthesis, and polyphosphate accumulates in acidocalcisomes, which are present in both bacteria and eukaryotic microbes (Komine et al., 2000; Rao et al., 2009). Based on studies of *S. cerevisiae*, the subunit of the complex responsible for polyphosphate kinase activity is Vtc4p. We recently identified a lesion in a gene encoding the *Chlamydomonas* putative VTC4 protein (au5.g9610 v4, Phytozome database g10027; Supplemental Figure 9), which has all of the conserved residues present in *S. cerevisiae* polyphosphate kinase.

The inability of *ars76* mutant cells to accumulate acidocalcisomes and polyphosphate during both S and N deprivation may impact various functionalities associated with energetics and regulation of cellular processes (Moreno and Docampo, 2013). We cannot discount the possibility that a regulatory function associated with polyphosphate biogenesis/degradation directly

impacts expression of both S- and N-responsive genes. Additionally, the *ars76* mutant may exhibit reduced fitness during nutrient deprivation if polyphosphate is a significant energy source generated and used during acclimation. However, vacuoles have a lower pH than the cytosol and likely function in the degradation of macromolecules such as proteins (Komine et al., 2000). Therefore, VTC proteins might be directly involved in fusing endocytic and autophagocytic vesicles with cargo destined for vacuolar degradation (Kim et al., 2012); in the absence of this capability, the cells would have a reduced capacity for acclimation, shortening the length of survival when nutrients become limiting. We have observed that Golgi can be positioned in cells contiguous to vacuoles, as also reported by Komine et al. (2000), where Golgi vesicles may fuse with vacuoles (Figure 5; Supplemental Figure 3). This raises the possibility that cargo from the Golgi may be transported to their final site of function following passage through vacuoles or developing acidocalcisomes.

METHODS

Strains, Growth Media, and Databases

Strain D66 (CC-4425; *cw15 nit2 mt+*) was used for the generation of insertional mutants (Pollock et al., 2005). The mutants were backcrossed at least three times to strain 21 gr (CC-1690 wt), which was used as our wild-type control strain (along with the rescued strain). The *ars11* mutant (CC-4275) is identical to *snrk2.1* (Gonzalez-Ballester et al., 2008); the strain was renamed previously to provide a functional descriptor of the gene. These strains can all be obtained from the Chlamydomonas Stock Center (http://chlamycollection.org). Tris acetate phosphate (TAP) medium was prepared based on a standard recipe (Gorman and Levine, 1965). S-depleted TAP medium (TAP-S) was prepared by substituting chloride salts for the SO_4^{2-} salts (Davies et al., 1994) and P-depleted medium (TA) was prepared by replacing potassium phosphate with potassium chloride (Moseley et al., 2009). Cultures were grown in 40 μmol photons m^{-2} s^{-1} constant light at room temperature and agitated at 200 rpm. N-depleted medium was prepared by omitting NH_4Cl from the Beijerinck's solution.

ARS and Phosphatase Assays

For evaluating the level of ARS activity associated with cells on solid medium, cells were maintained on TAP-S agar medium for 1 week prior to spraying colonies with a 10 mM solution of 5-bromo-4-chloro-3-indolyl sulfate (Sigma-Aldrich) in 0.1 M Tris-Cl, pH 7.5 (Davies et al., 1996). For performing phosphatase assays on solid medium, cells were maintained on TA agar medium for 1 week and the phosphatase assay was performed by application of 10 mM 5-bromo-4-chloro-3-indolyl phosphate (Sigma-Aldrich) onto the plates (Shimogawara et al., 1999).

Chlorophyll Determination

Chlorophyll measurements were made as described by Porra et al. (1989) after extraction of the pigments with methanol.

Rescue of the *ars76* Mutant Phenotype

Genes deleted or disrupted in the *ars76* mutant were identified on BAC 36J16 (PTQ 13789) and BAC 8B3 (PTQ 2889). DNA was isolated from *Escherichia coli* harboring the BACs using the Qiagen Maxi Prep Kit, and 3 to 5 μg of the isolated BAC DNA was digested with *Xba*I. We also digested 0.5 μg of plasmid pSP124S (harboring the Zeocin resistance marker gene) with *Bam*HI. The digested BAC and plasmid DNAs were mixed in an equal molar ratio and cotransformed into the backcrossed *ars76* mutant by electroporation (Shimogawara et al., 1998; Aksoy et al., 2013).

To specifically clone *VTC1*, the gene was amplified from BAC 36J16 with primers F (5′-CGCACAATTACGAGGCCAAACA-3′) and R (5′-CAGGATAGCTCTCGCGG GGAAA-3′) using Phusion High Fidelity Polymerase (New England Biolabs). The 3642-bp amplification product contained both the 5′ and 3′ untranslated regions of the gene. This product was A-tailed using Taq Polymerase (Qiagen) and ligated into pGEMT-E (Stratagene). The pGEMT-E plasmid (1 to 2 μg of DNA containing the *ARS76* gene) was then linearized with *Pst*I (Fermentas) and used for coelectroporation with 0.5 μg of *Bam*HI-digested pSP124S. Transformants generated with both the BAC and plasmid DNAs were selected on solid TAP agar medium containing 5 μg/mL Zeocin (Invitrogen) and then assayed for ARS activity to determine whether or not the mutant phenotype was rescued.

PCR and RT-qPCR

PCR was performed using Taq DNA polymerase (Qiagen) and 20 to 50 ng of genomic DNA template to assay for presence/absence of the *VTC1* gene. Primers P2-513065 (5′-TGCCATACAGATTTATCCGATG-3′) and stop-513065 (5′-GAAAAGGTAGTCAATGACGGCG-3′) amplify *VTC1* from its promoter to the end of third exon, producing a gene product of 1148 bp.

For RT-qPCR, total RNA was isolated using the RNeasy Plant Mini Kit (Qiagen) and treated with DNase I (Qiagen), as described in the RNeasy protocol, to remove any remaining genomic DNA. The purified RNA (0.5 to 1 μg) was also analyzed on formaldehyde agarose gels to determine sample quality. First-strand cDNA was generated by reverse transcription of 0.5 to 1 μg total RNA using the iScript cDNA Synthesis Kit (Bio-Rad). Real-time PCR in the Roche Light Cycler 480 was performed with the SensiMix NO-Rox SYBR Green I Kit as described by the manufacturer (Bioline). The samples generated by first-strand cDNA synthesis were diluted 1:50, and 5 μL was used as a template in PCR reactions (20 μL total) with 400 nM each of the forward and reverse primers. The primers sequences used for quantification are given in Supplemental Table 1. Reaction conditions were 10 min at 95°C, followed by 45 cycles of 95°C for 15 s, 60°C for 15 s, 72°C for 20 s, and a 5 s hold at 80°C to eliminate background fluorescence generated by the formation of primer dimers, followed by quantification of the fluorescence. Melt curve analyses were performed to determine whether or not the products represent a single amplified species. At least three biological replicates were analyzed for each experiment. Products were also analyzed by agarose gel electrophoresis.

Protein Analyses

A volume of culture containing 25 μg chlorophyll was pelleted and resuspended in 1 mL of HEPES buffer (5 mM HEPES and 10 mM EDTA, pH 7.5) containing the protease inhibitors 0.2 mM PMSF, 1 mM benzamidine, and 5 mM ε-aminocaproic acid (all from Sigma-Aldrich). The pellet was resuspended in 30 μL freezing solution (0.1 M DTT and 0.1 M sodium carbonate [Na_2CO_3], in HEPES buffer [as above]) and then flash frozen in liquid nitrogen. Cells were kept at −80°C until use. Prior to electrophoresis, samples, each containing 5 to 15 μg chlorophyll, were made to 2% SDS and 12.5% sucrose, boiled for 50 s, and then resolved by SDS-PAGE on a 10% polyacrylamide gel. Immunoblot analyses were performed as described previously (Aksoy et al., 2013). The dilution of LAO1 antibodies was 1:10,000 in 5% milk powder in TBS with 0.1% Tween.

Viability Assay

Cells were grown to mid-logarithmic phase (2 to 4 × 10^6 cells/mL) in liquid TAP medium prior to depriving the culture of S, P, or N. Cultures were first washed twice in medium devoid of S, P, or N and then resuspended in the same medium at the original culture volume. These cultures were maintained

in 40 μmol photons m^{-2} s^{-1} constant light at 25°C and agitated at 200 rpm. Five microliters of the culture was removed before and after various times of nutrient depleted growth and then deposited onto TAP medium to determine apparent cell viable as the culture became more and more starved for the nutrient. This enabled us to monitor cell viability following various periods of exposure to nutrient deprivation over a 6-week period.

Confocal Microscopy

Polyphosphate within cells was stained with DAPI and imaged through a 63× numerical aperture 1.3 glycerol immersion objective on a Leica SP5. DAPI was excited at 405 nm and emission was collected from 532 to 632 nm, similar to conditions previously described (Aschar-Sobbi et al., 2008; Gomez-Garcia et al., 2013). DAPI images are maximum intensity projections of stacks taken through the entire cell at 0.46-nm steps. Transmitted light images are single mid-plane sections.

Ultrastructure Analysis of Cells

For TEM, the cells were grown in TAP medium in which the Tris was replaced by 20 mM HEPES, pH 7.0. Cells were fixed in growth medium containing 1.25% glutaraldehyde (EM grade, from 50% stock; Polysciences) and 1% OsO_4 (from 4% stock; Electron Microscopy Sciences) for 1 h on ice. Samples were washed three times with growth medium and then the cells were resuspended in 20% BSA (w/v), incubated for 20 min at room temperature, centrifuged for 10 min at 16,000*g*, and the resulting pellet was incubated for 30 min at room temperature with 2.5% glutaraldehyde in the HEPES growth medium (as described above). After two washes with water, the cell pellet was cut into 1 to 2 mm^3 pieces and incubated in a 1% uranyl acetate aqueous solution at 4°C overnight. The pieces were washed two times with water, dehydrated in increasing concentrations of ethanol, and embedded in LR White resin (Polysciences) using ethanol as an intermediate solvent. The LR White resin was polymerized at 50°C for 3 d. Ultrathin sections (~60 nm) were cut with a diamond knife on a microtome and mounted onto Formvar-coated copper grids. Samples were contrasted with lead citrate (Reynolds, 1963), and images were acquired using a Jeol JEM-1400 transmission electron microscope.

Accession Numbers

Sequence data from this article can be found in the Phytozome database (www.phytozome.net) under the following accession numbers: *VTC1* (Cre12.g510250), *VTC4* (Cre02.g140700, alias g10027 and Cre09.g402775), *ECP56* (Cre17.g740800), *ECP61* (Cre09.g409300), *ECP76* (Cre06.g288550), and *ECP88* (Cre12.g556000).

Supplemental Data

The following materials are available in the online version of this article.

Supplemental Figure 1. Genetic Linkage Analysis of *AphVIII* Insertion and *ars*- Phenotype.

Supplemental Figure 2. Rescue of the *ars76* Mutant with the *VTC1* Gene (au5.g3279, Cre12.g510250).

Supplemental Figure 3. Vesicles Budding from Golgi (G) Fusing with Vacuoles (V) in a Section of a 21 gr Cell.

Supplemental Figure 4. Detection of Polyphosphate in wild-type 21 gr and *ars76* cells Grown in TAP (6×10^6 cells mL) with DAPI Staining.

Supplemental Figure 5. RNA-seq Data for Gene Model Cre12.g510250 (Encoding VTC1).

Supplemental Figure 6. Impact of Mutation on N Starvation Responses.

Supplemental Figure 7. Viability and Chlorophyll Determination of Cells after Transfer to –N Medium.

Supplemental Figure 8. RT-qPCR Analysis of Autophagy-Related Gene *ATG8*.

Supplemental Figure 9. Alignment of VTC Motifs of *Chlamydomonas* VTC4 (g100027) and *S. cerevisiae* Vtc4p.

Supplemental Table 1. Primers Used for RT-qPCR

ACKNOWLEDGMENTS

We thank Eva Nowack for help with the preparation of samples for TEM analysis, Heather Cartwright for help with confocal microscopy, and Alice Shieh for technical assistance during her summer internship. We also thank Devaki Bhaya and members of the Grossman and Bhaya Labs for helpful discussions. LAO1 antibody was a gift from Francis-André Wollman. This work was also in part supported by a U.S. Department of Energy grant awarded to A.R.G. (DE-FG02-12ER16338).

AUTHOR CONTRIBUTIONS

M.A. designed the research, performed research, analyzed data, and wrote the article. W.P. performed research. A.R.G. designed the research, analyzed data, and helped write the article.

Received July 9, 2014; revised August 25, 2014; accepted September 9, 2014; published October 3, 2014.

REFERENCES

Aksoy, M., Pootakham, W., Pollock, S.V., Moseley, J.L., González-Ballester, D., and Grossman, A.R. (2013). Tiered regulation of sulfur deprivation responses in *Chlamydomonas reinhardtii* and identification of an associated regulatory factor. Plant Physiol. **162:** 195–211.

Aschar-Sobbi, R., Abramov, A.Y., Diao, C., Kargacin, M.E., Kargacin, G.J., French, R.J., and Pavlov, E. (2008). High sensitivity, quantitative measurements of polyphosphate using a new DAPI-based approach. J. Fluoresc. **18:** 859–866.

Blaby, I.K., et al. (2013). Systems-level analysis of nitrogen starvation-induced modifications of carbon metabolism in a *Chlamydomonas reinhardtii* starchless mutant. Plant Cell **25:** 4305–4323.

Blaby-Haas, C.E., and Merchant, S.S. (2012). The ins and outs of algal metal transport. Biochim. Biophys. Acta **1823:** 1531–1552.

Bölling, C., and Fiehn, O. (2005). Metabolite profiling of *Chlamydomonas reinhardtii* under nutrient deprivation. Plant Physiol. **139:** 1995–2005.

Boyle, N.R., et al. (2012). Three acyltransferases and nitrogen-responsive regulator are implicated in nitrogen starvation-induced triacylglycerol accumulation in Chlamydomonas. J. Biol. Chem. **287:** 15811–15825.

Cakmak, T., Angun, P., Demiray, Y.E., Ozkan, A.D., Elibol, Z., and Tekinay, T. (2012a). Differential effects of nitrogen and sulfur deprivation on growth and biodiesel feedstock production of *Chlamydomonas reinhardtii*. Biotechnol. Bioeng. **109:** 1947–1957.

Cakmak, T., Angun, P., Ozkan, A.D., Cakmak, Z., Olmez, T.T., and Tekinay, T. (2012b). Nitrogen and sulfur deprivation differentiate lipid accumulation targets of *Chlamydomonas reinhardtii*. Bioengineered **3:** 343–346.

Ciaffi, M., Paolacci, A.R., Celletti, S., Catarcione, G., Kopriva, S., and Astolfi, S. (2013). Transcriptional and physiological changes in

the S assimilation pathway due to single or combined S and Fe deprivation in durum wheat (*Triticum durum* L.) seedlings. J. Exp. Bot. **64:** 1663–1675.

Cohen, A., Perzov, N., Nelson, H., and Nelson, N. (1999). A novel family of yeast chaperons involved in the distribution of V-ATPase and other membrane proteins. J. Biol. Chem. **274:** 26885–26893.

Collier, J.L., and Grossman, A.R. (1992). Chlorosis induced by nutrient deprivation in *Synechococcus* sp. strain PCC 7942: not all bleaching is the same. J. Bacteriol. **174:** 4718–4726.

Davies, J.P., Yildiz, F., and Grossman, A.R. (1994). Mutants of Chlamydomonas with aberrant responses to sulfur deprivation. Plant Cell **6:** 53–63.

Davies, J.P., Yildiz, F.H., and Grossman, A. (1996). Sac1, a putative regulator that is critical for survival of *Chlamydomonas reinhardtii* during sulfur deprivation. EMBO J. **15:** 2150–2159.

Davies, J.P., Yildiz, F.H., and Grossman, A.R. (1999). Sac3, an Snf1-like serine/threonine kinase that positively and negatively regulates the responses of *Chlamydomonas* to sulfur limitation. Plant Cell **11:** 1179–1190.

de Hostos, E.L., Togasaki, R.K., and Grossman, A. (1988). Purification and biosynthesis of a derepressible periplasmic arylsulfatase from *Chlamydomonas reinhardtii.* J. Cell Biol. **106:** 29–37.

Ding, B., Zhang, G., Yang, X., Zhang, S., Chen, L., Yan, Q., Xu, M., Banerjee, A.K., and Chen, M. (2014). Phosphoprotein of human parainfluenza virus type 3 blocks autophagosome-lysosome fusion to increase virus production. Cell Host Microbe **15:** 564–577.

Freimoser, F.M., Hürlimann, H.C., Jakob, C.A., Werner, T.P., and Amrhein, N. (2006). Systematic screening of polyphosphate (poly P) levels in yeast mutant cells reveals strong interdependence with primary metabolism. Genome Biol. **7:** R109.

Ghirardi, M.L., Posewitz, M.C., Maness, P.C., Dubini, A., Yu, J., and Seibert, M. (2007). Hydrogenases and hydrogen photoproduction in oxygenic photosynthetic organisms. Annu. Rev. Plant Biol. **58:** 71–91.

Giovanelli, J., Mudd, S.H., and Datko, A.H. (1985). Quantitative analysis of pathways of methionine metabolism and their regulation in lemna. Plant Physiol. **78:** 555–560.

Gomez-Garcia, M.R., Fazeli, F., Grote, A., Grossman, A.R., and Bhaya, D. (2013). Role of polyphosphate in thermophilic *Synechococcus* sp. from microbial mats. J. Bacteriol. **195:** 3309–3319.

Gonzalez-Ballester, D., Pollock, S.V., Pootakham, W., and Grossman, A.R. (2008). The central role of a SNRK2 kinase in sulfur deprivation responses. Plant Physiol. **147:** 216–227.

González-Ballester, D., Casero, D., Cokus, S., Pellegrini, M., Merchant, S.S., and Grossman, A.R. (2010). RNA-seq analysis of sulfur-deprived Chlamydomonas cells reveals aspects of acclimation critical for cell survival. Plant Cell **22:** 2058–2084.

Gorman, D.S., and Levine, R.P. (1965). Cytochrome f and plastocyanin: their sequence in the photosynthetic electron transport chain of *Chlamydomonas reinhardi.* Proc. Natl. Acad. Sci. USA **54:** 1665–1669.

Hothorn, M., et al. (2009). Catalytic core of a membrane-associated eukaryotic polyphosphate polymerase. Science **324:** 513–516.

Hsieh, S.I., Castruita, M., Malasarn, D., Urzica, E., Erde, J., Page, M.D., Yamasaki, H., Casero, D., Pellegrini, M., Merchant, S.S., and Loo, J.A. (2013). The proteome of copper, iron, zinc, and manganese micronutrient deficiency in *Chlamydomonas reinhardtii.* Mol. Cell. Proteomics **12:** 65–86.

Irihimovitch, V., and Stern, D.B. (2006). The sulfur acclimation SAC3 kinase is required for chloroplast transcriptional repression under sulfur limitation in *Chlamydomonas reinhardtii*. Proc. Natl. Acad. Sci. USA **103:** 7911–7916.

Kim, S.H., Kwon, C., Lee, J.H., and Chung, T. (2012). Genes for plant autophagy: functions and interactions. Mol. Cells **34:** 413–423.

Komine, Y., Eggink, L.L., Park, H., and Hoober, J.K. (2000). Vacuolar granules in *Chlamydomonas reinhardtii*: polyphosphate and a 70-kDa polypeptide as major components. Planta **210:** 897–905.

Komsic-Buchmann, K., Stephan, L.M., and Becker, B. (2012). The SEC6 protein is required for contractile vacuole function in *Chlamydomonas reinhardtii.* J. Cell Sci. **125:** 2885–2895.

Kopriva, S., Mugford, S.G., Baraniecka, P., Lee, B.R., Matthewman, C.A., and Koprivovam, A. (2012). Control of sulfur partitioning between primary and secondary metabolism in Arabidopsis. Front. Plant Sci. **3:** 163.

Kopriva, S., Mugford, S.G., Matthewman, C., and Koprivova, A. (2009). Plant sulfate assimilation genes: redundancy versus specialization. Plant Cell Rep. **28:** 1769–1780.

Lee, B.R., et al. (2012). Effects of fou8/fry1 mutation on sulfur metabolism: is decreased internal sulfate the trigger of sulfate starvation response? PLoS One **7:** e39425.

Lewandowska, M., and Sirko, A. (2008). Recent advances in understanding plant response to sulfur-deficiency stress. Acta Biochim. Pol. **55:** 457–471.

Lunde, C., Zygadlo, A., Simonsen, H.T., Nielsen, P.L., Blennow, A., and Haldrup, A. (2008). Sulfur starvation in rice: the effect on photosynthesis, carbohydrate metabolism, and oxidative stress protective pathways. Physiol. Plant. **134:** 508–521.

Maruyama-Nakashita, A., Inoue, E., Watanabe-Takahashi, A., Yamaya, T., and Takahashi, H. (2003). Transcriptome profiling of sulfur-responsive genes in Arabidopsis reveals global effects of sulfur nutrition on multiple metabolic pathways. Plant Physiol. **132:** 597–605.

Miller, R., et al. (2010). Changes in transcript abundance in *Chlamydomonas reinhardtii* following nitrogen deprivation predict diversion of metabolism. Plant Physiol. **154:** 1737–1752.

Moreno, S.N., and Docampo, R. (2013). Polyphosphate and its diverse functions in host cells and pathogens. PLoS Pathog. **9:** e1003230.

Moseley, J.L., and Grossman, A.R. (2009). Phosphate metabolism and responses to phosphorous deficiency. In The *Chlamydomonas* Sourcebook. E.H. Harris, D. Stern, and G.G. Witman, eds (Amsterdan: Elsevier), pp. 189–216.

Moseley, J.L., Chang, C.W., and Grossman, A.R. (2006). Genome-based approaches to understanding phosphorus deprivation responses and PSR1 control in *Chlamydomonas reinhardtii.* Eukaryot. Cell **5:** 26–44.

Moseley, J.L., Gonzalez-Ballester, D., Pootakham, W., Bailey, S., and Grossman, A.R. (2009). Genetic interactions between regulators of Chlamydomonas phosphorus and sulfur deprivation responses. Genetics **181:** 889–905.

Müller, O., Neumann, H., Bayer, M.J., and Mayer, A. (2003). Role of the Vtc proteins in V-ATPase stability and membrane trafficking. J. Cell Sci. **116:** 1107–1115.

Müller, O., Bayer, M.J., Peters, C., Andersen, J.S., Mann, M., and Mayer, A. (2002). The Vtc proteins in vacuole fusion: coupling NSF activity to V(0) trans-complex formation. EMBO J. **21:** 259–269.

Nguyen, A.V., Thomas-Hall, S.R., Malnoe, A., Timmins, M., Mussgnug, J.H., Rupprecht, J., Kruse, O., Hankamer, B., and Schenk, P.M. (2008). Transcriptome for photobiological hydrogen production induced by sulfur deprivation in the green alga *Chlamydomonas reinhardtii*. Eukaryot. Cell **7:** 1965–1979.

Nikiforova, V.J., Daub, C.O., Hesse, H., Willmitzer, L., and Hoefgen, R. (2005a). Integrative gene-metabolite network with implemented causality deciphers informational fluxes of sulphur stress response. J. Exp. Bot. **56:** 1887–1896.

Nikiforova, V.J., Kopka, J., Tolstikov, V., Fiehn, O., Hopkins, L., Hawkesford, M.J., Hesse, H., and Hoefgen, R. (2005b). Systems

rebalancing of metabolism in response to sulfur deprivation, as revealed by metabolome analysis of Arabidopsis plants. Plant Physiol. **138:** 304–318.

Ogawa, N., DeRisi, J., and Brown, P.O. (2000). New components of a system for phosphate accumulation and polyphosphate metabolism in *Saccharomyces cerevisiae* revealed by genomic expression analysis. Mol. Biol. Cell **11:** 4309–4321.

Page, M.D., Allen, M.D., Kropat, J., Urzica, E.I., Karpowicz, S.J., Hsieh, S.I., Loo, J.A., and Merchant, S.S. (2012). Fe sparing and Fe recycling contribute to increased superoxide dismutase capacity in iron-starved *Chlamydomonas reinhardtii.* Plant Cell **24:** 2649–2665.

Pérez-Pérez, M.E., Florencio, F.J., and Crespo, J.L. (2010). Inhibition of target of rapamycin signaling and stress activate autophagy in *Chlamydomonas reinhardtii.* Plant Physiol. **152:** 1874–1888.

Pollock, S.V., Pootakham, W., Shibagaki, N., Moseley, J.L., and Grossman, A.R. (2005). Insights into the acclimation of *Chlamydomonas reinhardtii* to sulfur deprivation. Photosynth. Res. **86:** 475–489.

Pootakham, W., Gonzalez-Ballester, D., and Grossman, A.R. (2010). Identification and regulation of plasma membrane sulfate transporters in Chlamydomonas. Plant Physiol. **153:** 1653–1668.

Porra, R.J., Thomson, W.A., and Kriedman, P.E. (1989). Determination of accurate extinction coefficients and simultaneous equations for assaying chlorophylls a and b extracted with four different solvents: verification of the concentration of chlorophyll standards by aatomic absorption spectroscopy. Biochim. Biophys. Acta **975:** 384–394.

Quisel, J.D., Wykoff, D.D., and Grossman, A.R. (1996). Biochemical characterization of the extracellular phosphatases produced by phosphorus-deprived *Chlamydomonas reinhardtii.* Plant Physiol. **111:** 839–848.

Rao, N.N., Gómez-García, M.R., and Kornberg, A. (2009). Inorganic polyphosphate: essential for growth and survival. Annu. Rev. Biochem. **78:** 605–647.

Ravina, C.G., Barroso, C., Vega, J.M., and Gotor, C. (1999). Cysteine biosynthesis in *Chlamydomonas reinhardtii*. Molecular cloning and regulation of O-acetylserine(thiol)lyase. Eur. J. Biochem. **264:** 848–853.

Ravina, C.G., Chang, C.I., Tsakraklides, G.P., McDermott, J.P., Vega, J.M., Leustek, T., Gotor, C., and Davies, J.P. (2002). The *sac* mutants of *Chlamydomonas reinhardtii* reveal transcriptional and posttranscriptional control of cysteine biosynthesis. Plant Physiol. **130:** 2076–2084.

Reynolds, E.S. (1963). The use of lead citrate at high pH as an electron-opaque stain in electron microscopy. J. Cell Biol. **17:** 208–212.

Schmollinger, S., et al. (2014). Nitrogen-sparing mechanisms in Chlamydomonas affect the transcriptome, the proteome, and photosynthetic metabolism. Plant Cell **26:** 1410–1435.

Shimogawara, K., Fujiwara, S., Grossman, A., and Usuda, H. (1998). High-efficiency transformation of *Chlamydomonas reinhardtii* by electroporation. Genetics **148:** 1821–1828.

Shimogawara, K., Wykoff, D.D., Usuda, H., and Grossman, A.R. (1999). *Chlamydomonas reinhardtii* mutants abnormal in their responses to phosphorus deprivation. Plant Physiol. **120:** 685–694.

Takahashi, H., Braby, C.E., and Grossman, A.R. (2001). Sulfur economy and cell wall biosynthesis during sulfur limitation of *Chlamydomonas reinhardtii.* Plant Physiol. **127:** 665–673.

Tenenboim, H., Smirnova, J., Willmitzer, L., Steup, M., and Brotman, Y. (2014). VMP1-deficient Chlamydomonas exhibits severely aberrant cell morphology and disrupted cytokinesis. BMC Plant Biol. **14:** 121.

Urzica, E.I., Adler, L.N., Page, M.D., Linster, C.L., Arbing, M.A., Casero, D., Pellegrini, M., Merchant, S.S., and Clarke, S.G. (2012). Impact of oxidative stress on ascorbate biosynthesis in Chlamydomonas via regulation of the VTC2 gene encoding a GDP-L-galactose phosphorylase. J. Biol. Chem. **287:** 14234–14245.

Urzica, E.I., Vieler, A., Hong-Hermesdorf, A., Page, M.D., Casero, D., Gallaher, S.D., Kropat, J., Pellegrini, M., Benning, C., and Merchant, S.S. (2013). Remodeling of membrane lipids in iron-starved Chlamydomonas. J. Biol. Chem. **288:** 30246–30258.

Uttenweiler, A., Schwarz, H., Neumann, H., and Mayer, A. (2007). The vacuolar transporter chaperone (VTC) complex is required for microautophagy. Mol. Biol. Cell **18:** 166–175.

Werner, T.P., Amrhein, N., and Freimoser, F.M. (2007). Inorganic polyphosphate occurs in the cell wall of *Chlamydomonas reinhardtii* and accumulates during cytokinesis. BMC Plant Biol. **7:** 51.

Wykoff, D.D., Davies, J.P., Melis, A., and Grossman, A.R. (1998). The regulation of photosynthetic electron transport during nutrient deprivation in *Chlamydomonas reinhardtii.* Plant Physiol. **117:** 129–139.

Yehudai-Resheff, S., Zimmer, S.L., Komine, Y., and Stern, D.B. (2007). Integration of chloroplast nucleic acid metabolism into the phosphate deprivation response in *Chlamydomonas reinhardtii.* Plant Cell **19:** 1023–1038.

Yildiz, F.H., Davies, J.P., and Grossman, A.R. (1994). Characterization of sulfate transport in *Chlamydomonas reinhardtii* during sulfur-limited and sulfur-sufficient growth. Plant Physiol. **104:** 981–987.

Zhang, L., Happe, T., and Melis, A. (2002). Biochemical and morphological characterization of sulfur-deprived and H_2-producing *Chlamydomonas reinhardtii* (green alga). Planta **214:** 552–561.

Zhang, Z., Shrager, J., Jain, M., Chang, C.W., Vallon, O., and Grossman, A.R. (2004). Insights into the survival of *Chlamydomonas reinhardtii* during sulfur starvation based on microarray analysis of gene expression. Eukaryot. Cell **3:** 1331–1348.